Shallow Salinity Minima in the North Pacific

XIAOJUN YUAN AND LYNNE D. TALLEY

Scripps Institution of Oceanography, La Jolla, California

(Manuscript received 28 November 1990, in final form 18 February 1992)

ABSTRACT

CTD/STD data from 24 cruises in the North Pacific are studied for their vertical salinity structure and compared to bottle observations. A triple-salinity minimum is found in two separated regions in the eastern North Pacific. In the first region, bounded by the northern edge of the subarctic frontal zone and the 34°N front between 160° and 150°W, a middle salinity minimum is found below the permanent pycnocline in the density range of 26.0 and 26.5 σ_θ. This middle minimum underlies Reid's shallow salinity minimum and overlies the North Pacific Intermediate Water (NPIW). In the second region, southeast of the first, a seasonal salinity minimum appears above the shallow salinity minimum at densities lower than 25.1 σ_θ. The shallow salinity minimum and the NPIW can be found throughout year, while the seasonal minimum only appears in summer and fall.

The middle and shallow salinity minima, as well as the seasonal minimum, originate at the sea surface in the northeast Pacific. The properties at the minima depend on the surface conditions in their source areas. The source of the middle minimum is the winter surface water in a narrow band between the gyre boundary and the subarctic front west of 170°W. The shallow salinity minimum is generated in winter and is present throughout the year. The seasonal salinity minimum has the same source area as the shallow salinity minimum but is formed in summer and fall at lower density and is not present in winter.

A tropical shallow salinity minimum found south of 18°N does not appear to be connected with the shallow salinity minimum in the eastern North Pacific. South of 20°N, the shallow salinity minimum and the NPIW appear to merge into a thick, low salinity water mass. When an intrusion of high salinity water breaks through this low salinity water mass south of 18°N, this tropical salinity minimum appears at the same density as the shallow salinity minimum. Though the water mass of the tropical minimum is derived from the water in the shallow salinity minimum, the formation of the vertical minimum is different.

1. Introduction

Vertical salinity minima in the North Pacific have been the subject of much study since Wüst (1930) noted the presence of a widespread minimum in the subtropics. Two large-scale salinity minima have been described. The North Pacific Intermediate Water (NPIW), indicated by a well-defined, thick and smooth salinity minimum, occurs in the density range of 26.7 to 26.9 σ_θ throughout the subtropics where potential vorticity suggests wind-driven circulation (Talley 1992). According to Reid (1965), vertical mixing transmits cold, less saline, and oxygen-rich water through the pycnocline in the subarctic gyre. Lateral mixing along isopycnals and the general circulation then carry these characteristics equatorward from the subarctic gyre to the subtropical gyre. More recently, Talley (1991) examined the details of this process and suggested that freshening and oxygenation at the NPIW densities occur primarily in the Okhotsk Sea through brine rejection below sea-ice formation (Kitani 1973). Formation of the actual NPIW salinity minimum occurs when Oyashio and modified Kuroshio waters meet in the mixed water region east of Hokkaido (Hasunuma 1978; Talley 1992).

The "shallow salinity minimum" (SSM) is observed at $25.1 < \sigma_\theta < 26.2$ in the eastern Pacific south of 50°N (Reid 1973) and above the NPIW. It spreads over the eastern boundary current region and turns to the southwest around 25°N following the current. At lower latitudes, the shallow salinity minimum is found from 130°W to the western boundary between 10°N and the equator. Tsuchiya (1982) suggested that the source of the SSM is surface water of low salinity and high oxygen concentration near 35°–50°N, 145°–160°W. This surface water is advected equatorward in the eastern part of the subtropical gyre and meets more saline but less dense subtropical surface water. Saline surface water from the west and evaporation at the surface result in a subsurface salinity minimum (Reid 1973; Tsuchiya 1982). Talley (1985), using a modified LPS model (Luyten et al. 1983), showed that the SSM can result from the wind-driven, ventilated circulation in the subtropical gyre. The density and salinity of the minimum vary as a result of sea surface conditions in

Corresponding author address: Ms. Xiaojun Yuan, Scripps Institution of Oceanography, 0230, 9500 Gilman Dr., La Jolla, CA 92093-0230.

the source region, and the density range extends to the highest density that outcrops in the subtropical gyre.

The above studies of the two salinity minima were based on the historical hydrographic bottle data. The newer technology of STD and CTD profiling has provided data with high vertical resolution since the late 1960s. For example, the detailed salinity distribution from a CTD section from Hawaii to Alaska along 152°W is examined in section 2. A third salinity minimum is reported in the present work, which is found above the NPIW and below the SSM within and south of the subarctic frontal zone (SFZ). To find the horizontal extent of this triple salinity minimum, STD/CTD data from 24 cruises in the North Pacific are used. Salinity minima are selected from these data and mapped on four isopycnals (section 3). The triple salinity minimum is found in two separate regions. In the first, a middle salinity minimum occurs in the density range of 26.2 to 26.5 σ_θ, which is below the conventional SSM. This minimum usually appears as a sharp intrusion below the pycnocline. In the second, a seasonal minimum (summer and fall) lies above the SSM. Both seasonal and shallow salinity minima have a broad density range. Possible source areas for these salinity minima are suggested in section 4 based on observations. The processes of subduction are discussed from theoretical points of view in section 6. In section 5, a shallow salinity minimum in the tropics is shown to differ from the SSM in the subtropical gyre. The formation of this minimum cannot be explained by ventilation theory. It is likely to be formed by intrusion of high salinity eastern equatorial water at densities greater than 26.0 σ_θ into a thick, low salinity, subsurface water.

2. Salinity minima along 152°W

The second leg of the Marathon Expedition (Marathon II) proceeded from Hawaii to Alaska along 152°W during May 1984 (Fig. 1). Pressure, temperature, and salinity at 98 stations were measured continuously with a CTD. After calibration and block-averaging, the final data were reported every 2 db. Station separation varied from 14.4 km near the Alaska coast to 60.7 km in the middle of the gyre. Details of data collection and processing can be found in Martin et al. (1987), and the basic hydrography is described in Talley et al. (1991). Our attention is focused on significant salinity intrusions found south of the subarctic front, in which the vertical scale is at least 50 m and the horizontal scale is relatively large. Features caused by microscale turbulence and local surface influence are beyond the scope of this paper. We therefore smooth the data further with a Gaussian filter. Figure 2 shows experiments with total filter widths of 20, 30, and 40 m (from left to right). The resulting vertical salinity distributions from station 50 are in the upper panels. The salinity minima from 35° to 45°N are

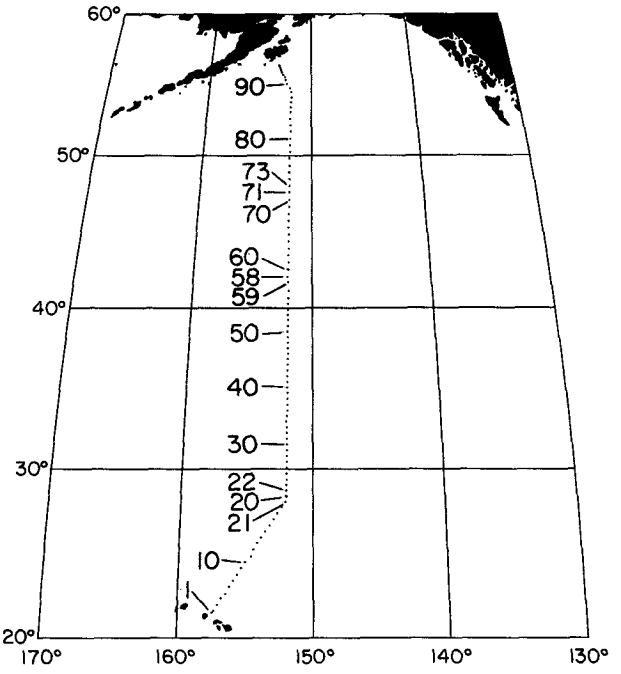

FIG. 1. Hydrographic section occupied on the second leg of the Marathon expedition (R/V *T. Washington*) in May 1984. The dots are the station locations.

identified from filtered data by computer and plotted versus density in the bottom panels of Fig. 2. The arrows indicate station 50. Based on the panels, there are three significant minima at station 50. With a 20-m filter (left column), seven minima are found. With a 30-m filter, four minima are selected. With the 40-m filter, three minima are selected. These three minima are not eliminated with 50- and 60-m smoothing (not shown here). Based on this example and many others, smoothing with a Gaussian filter of 40-m width was chosen for this research.

The western side of the SSM at middle latitudes and its source water region at high latitudes (see Fig. 1 in Reid 1973) were crossed by the Marathon II cruise. The distributions of salinity, temperature, and σ_θ along the cruise track from stations 19 to 80 are plotted for the upper 800 m in Fig. 3. The salinity in this section shows a strong halocline at about 100-m depth north of 39°N. The subarctic frontal zone (SFZ) lies between stations 52 and 58, which is the southern end of the halocline and separates the less-saline subarctic water from relatively high salinity subtropical water (Fig. 3a). A weak temperature front occurs in the SFZ (Fig. 3b). No significant surface density front occurs in the SFZ since temperature and salinity compensate each other in the mixed layer. Farther south, the "34°N front" [also called the "northern subtropical front" by Lynn (1986)] is found just south of 34°N between stations 36 and 37 in both salinity and temperature. The subtropical frontal zone, which is the northern boundary

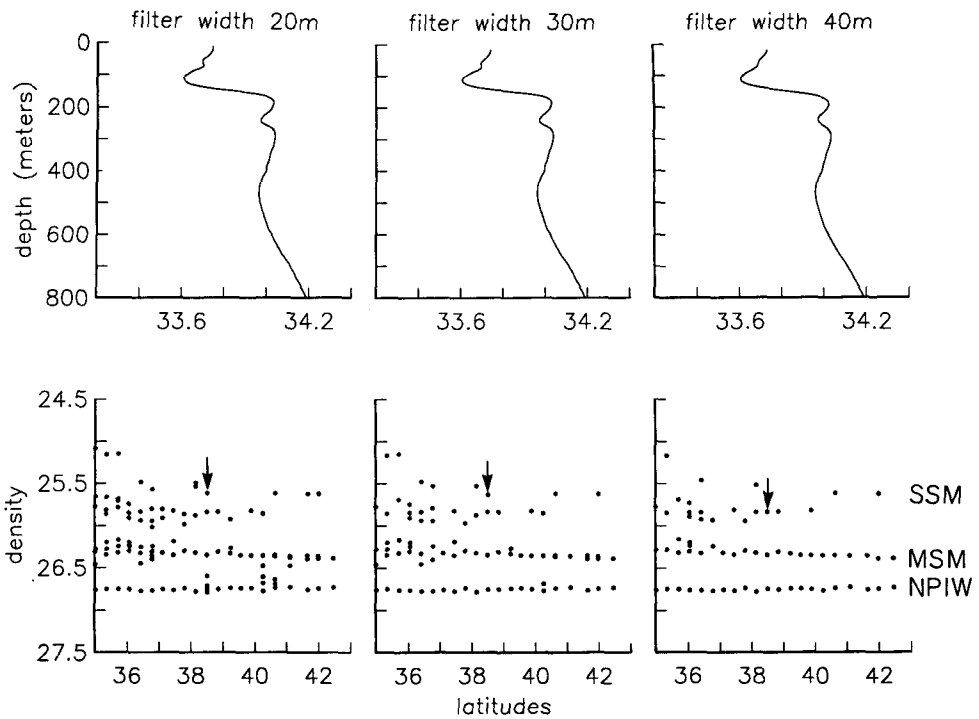

FIG. 2. Gaussian-filtering experiments. Upper panel: Vertical distribution of salinity at station 50 (38.5°N). Bottom panel: The salinity minima selected from filtered data versus density from 35° to 43°N. From left to right, applied filter widths are 20, 30, and 40 m, respectively. Arrows indicate the location of station 50.

of the North Pacific Central Water (Roden 1980), is located between stations 27 and 31.

All salinity minima are selected from the smoothed data and superimposed on the property distributions in Fig. 3. There are three groups of minima along 152°W. The NPIW, indicated by crosses, starts from the subpolar gyre and extends south of the subtropical frontal zone. The depth of the NPIW increases southward from about 200 m north of the SFZ to about 600 m south of the subtropical frontal zone. The SSM occurs near the base of the mixed layer. Represented by circles in Fig. 3, this minimum begins near 50°N and ends at the subtropical front. The depth of the SSM is less than 100 m north of the 34°N front and greater than 100 m south of the front. North of the 34°N front, the SSM is more or less in the mixed layer. South of the 34°N front, the SSM extends downward and lies well below the mixed layer.

There is another group of minima between the NPIW and the SSM, which we call the "middle salinity minimum" and indicate by asterisks in Fig. 3. The middle salinity minimum appears below the halocline and the pycnocline. It starts from the base of the pycnocline at 43°N, which is the northern edge of the SFZ, crosses the frontal zone and extends into the subtropical gyre as far as 34°N. South of the 34°N front, the minimum gradually disappears. Although some minima can be identified farther south, they are not significant. Salinity versus density plotted in Fig. 4 from stations 30 to 80 helps to verify this. The three salinity minima are connected by dashed lines for identification. The top dashed line connects the SSM, and so on. The middle salinity minimum is found between stations 38 and 61. It extends 1875 km in the horizontal. South of station 38 (34°N front), the minimum becomes harder to identify. The density range of the middle salinity minimum is mainly between 26.2 and 26.4 σ_θ. The SSM is observed at most of the stations in Fig. 4. The density, depth, and strength of the SSM vary from station to station. The density range of the minimum is from 25.1 to 26.0 σ_θ. The NPIW, characterized by the thick and smooth salinity minimum, occurs in the density range of 26.7 to 26.8 σ_θ at most of the stations, except those north of the SFZ.

Figure 5 shows the salinity and temperature at the three salinity minima along 152°W. Salinity at the NPIW is nearly uniform at about 34.0 psu (practical salinity units) south of 43°N. The salinity at the SSM occurs in a wide range from 32.5 to 34.5 psu. The range of salinity at the middle salinity minimum is from 33.9 to 34.2 psu, which is much smaller than at the SSM. The temperature also does not change much across the section at the NPIW. The temperature at both the shallow and middle salinity minima decreases northwards. The rate of decrease is slightly larger at the SSM than at the middle minimum.

The SSM Reid (1973) described has density lower than 26.0 σ_θ and salinity approximately 33.5 psu near

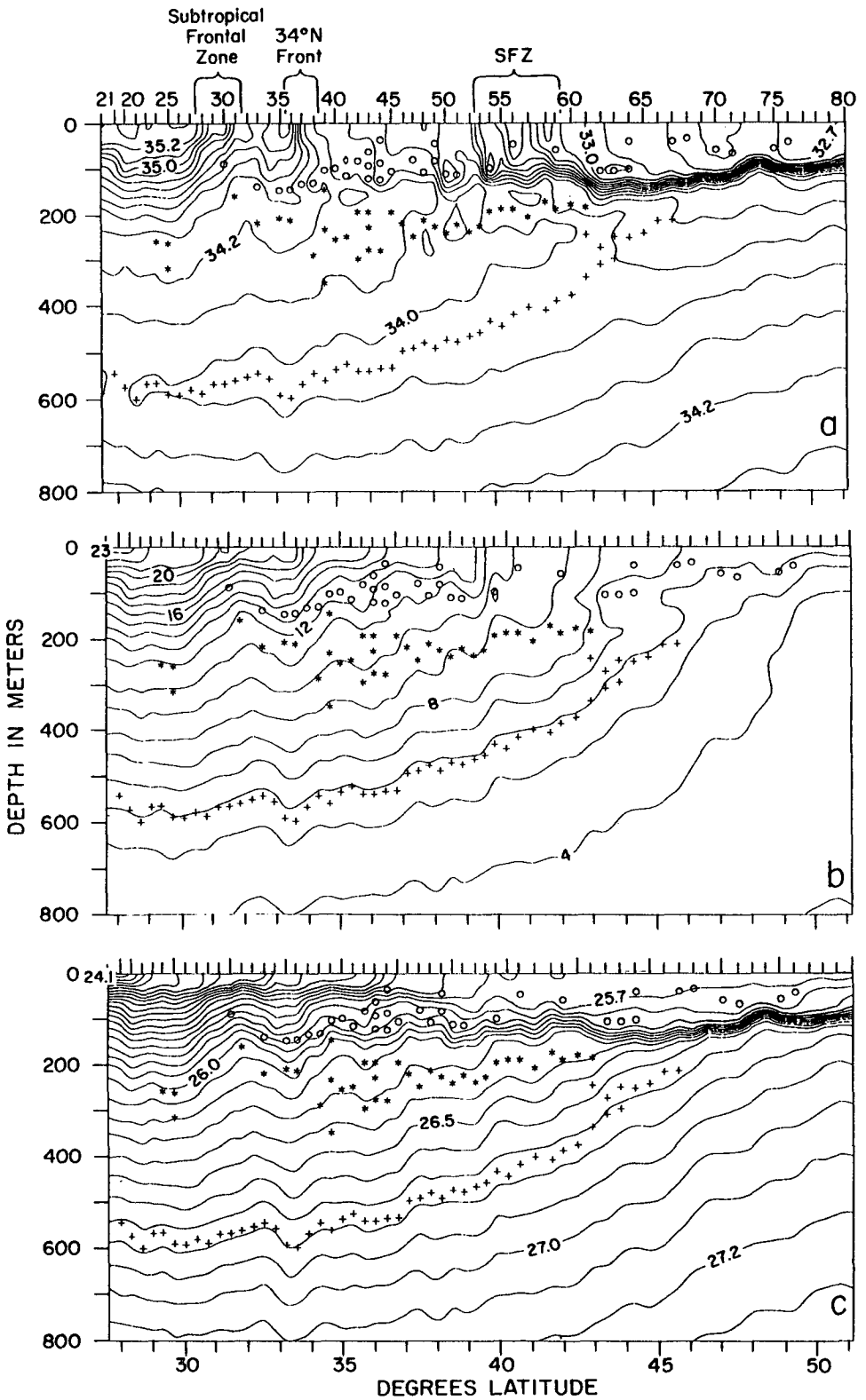

FIG. 3. Meridional section from Marathon II (152°W) between stations 19 and 80. Crosses, asterisks, and circles indicate the NPIW, middle, and shallow salinity minima, respectively. Panels are (a) salinity, (b) temperature, and (c) σ_θ.

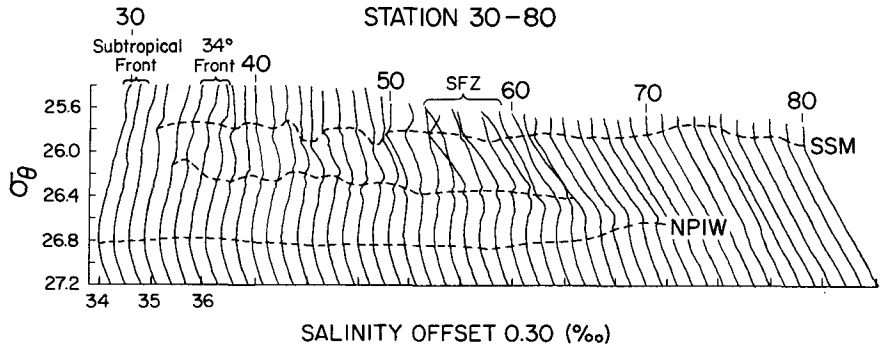

FIG. 4. Salinity versus potential density from stations 30–80 of the Marathon II cruise (152°W). Salinity is correct at station 30 and offset by 0.30 psu on each subsequent station.

the SFZ around 150°W. Based on the information given above, we are convinced that the SSM on the Marathon II section corresponds to Reid's SSM. The middle salinity minimum on the Marathon II is a newly observed phenomenon, relying on CTD profiles for its identification. The middle salinity minimum has four significant characteristics. First, the minimum starts at the northern end of SFZ and extends southward until it reaches the 34°N front. Thus, we suspect that the minimum is related to frontal activity and contributes to the water exchange between the subarctic and subtropical gyres. Second, the minimum occurs over a limited density range (26.1 to 26.4 σ_θ along this section). These isopycnals are below the pycnocline, while the SSM is above or within the pycnocline north of the 34°N front. Third, the strength and vertical scale of the middle salinity minimum do not change significantly from station to station within the frontal zone (Fig. 4), but the minimum is much thinner and less uniform than the NPIW and also less variable than the SSM. The vertical scale of this minimum is less than 100 m. Last, the shape of the minimum in σ_θ/S is very sharp (Fig. 6). This implies that the minimum is caused by a strong new intrusion that has not yet been eroded significantly by vertical turbulent mixing or double diffusion. All these characteristics distinguish the middle salinity minimum from the SSM and the NPIW.

The triple salinity minimum within and south of the SFZ found in the Marathon II data suggests the following questions. How many salinity minima are commonly found in the North Pacific? Is the triple-salinity minimum a time-dependent phenomenon? What is its horizontal extent? What and where are the sources of these minima? A larger collection of CTD/STD data is used to address these issues in the following sections.

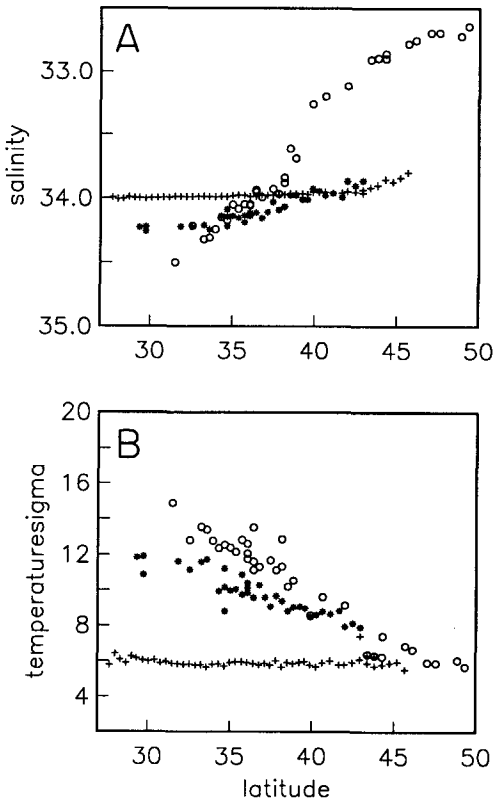

FIG. 5. (a) Salinity and (b) temperature at the three salinity minima in Marathon II from stations 19 to 80.

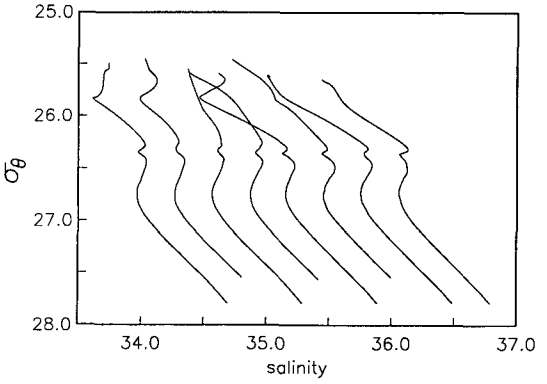

FIG. 6. The σ_θ/S relations at Marathon II stations 50–57, which cross the subarctic frontal zone at 152°W in May 1984.

TABLE 1. CTD and STD cruises used in this research. Providers' names are listed in the reference column when there are no available references for the data.

Ship	Stations	Survey period	Reference
R/V *Thomas G. Thompson*	133	Apr 1968	Roden (1970)
R/V *Thomas G. Thompson*	249	Nov–Dec 1969	Roden, G.
R/V *Thomas G. Thompson*	270	Mar–May 1971	Roden (1972)
R/V *Thomas G. Thompson*	300	Sep–Nov 1972	Roden (1974)
R/V *Thomas G. Thompson*	257	Jan–Feb 1974	Roden (1980)
R/V *Thomas G. Thompson*	287	Sep–Oct 1975	Roden (1977)
David Starr Jordan	118	Jun 1976	Lynn (1986)
R/V *Thomas G. Thompson*	122	Jan–Feb 1980	Roden (1980)
R/V *Thomas Washington*	24	May 1981	Niiler et al. (1985)
R/V *Thomas Washington*	40	Jun 1981	Joyce, T.
USNS *Silas Bent*	51	Sep 1982	Teague (1983)
R/V *Thomas G. Thompson*	27	May–Jun 1982	Joyce, T.
R/V *Thomas G. Thompson*	45	Jul–Aug 1982	Joyce, T.
R/V *Thomas G. Thompson*	17	Jul 1983	Niiler (1986)
R/V *Thomas G. Thompson*	52	Sep–Nov 1983	Joyce (1987)
R/V *Thomas G. Thompson*	28	Nov–Dec 1983	Joyce, T.
R/V *Thomas Washington*	98	May 1984	Martin et al. (1987)
R/V *Thomas G. Thompson*	55	Sep–Oct 1984	Joyce (1987)
R/V *Thomas G. Thompson*	216	Mar–Jun 1985	Roemmich et al. (1990)
R/V *Thomas G. Thompson*	115	Aug–Sep 1985	Talley et al. (1988)
R/V *Melville*	10	May 1987	Worcester, P.
NOAA ship *Oceanographer*	16	Sep 1987	Worcester, P.
R/V *Thomas Washington*	22	Jun 1981	Warren and Owens (1988)
R/V *Thomas Washington*	123	Jun–Jul 1991	WOCE P17

3. Salinity minima in the North Pacific

Table 1 lists the 24 CTD/STD cruises in the North Pacific used in this section. Most of the surveys were conducted north of 20°N. The profiles were vertically smoothed with a Gaussian filter of 40 m total width prior to identification of the salinity minima.

Based on the vertical salinity profiles at most stations, minima at the NPIW density and less can be separated into four density layers: density less than 25.1 σ_θ, 25.1–26 σ_θ, 26.0 to 26.5 σ_θ, and 26.5 to 26.8 σ_θ. The horizontal extent of the salinity minima in the four density layers is shown in Fig. 7. The groups of stations that show the vertical minima in corresponding density layers are shaded. All of the minima except the NPIW (in Fig. 7d) occur only in the eastern North Pacific, similar to Reid's (1973) SSM.

The salinity minimum that is less dense than 25.1 σ_θ (Fig. 7a) occurs only in summer and fall, such as in July 1976, November 1969, September 1972, September 1975, and June 1991. The data taken on the cruises of January–February 1968, 1974, and 1980 and April 1983 do not show any minimum in this density range since the surface density in winter is not less than 25.1 σ_θ in most of the area. Therefore, we call it a "seasonal salinity minimum." The horizontal extent in Fig. 7a is artificially confined by the limited summer and fall data coverage.

In the layer 25.1 to 26.0 σ_θ (Fig. 7b), the salinity minimum starts from 45°N, 160°W and spreads over the eastern boundary current region. It can be found in all seasons and occupies most of Reid's SSM area. The densities of Reid's SSM correspond to this density range. There is a separate region of minima south of 20°N around 140°W based on the data collected during September–November 1972 and June–July 1991. This minimum, even though it occurs in the same density range, does not seem to be a continuation of the northern part of the SSM. It will be discussed again in section 5.

Figure 7c shows the salinity minimum in the density range of 26.0 to 26.5 σ_θ. The minimum usually occurs below the permanent pycnocline. The horizontal extent of the minimum in our data is bounded by the northern edge of the SFZ and the 34°N front between 160° and 150°W. The scattered patches may imply that this minimum can spread as far as 31°N, 137°W, but we do not have enough data to prove this. The minimum is also found in different seasons, such as September 1975, September 1983, May 1984, and May and September 1987, but not in September 1982 in the same area. The vertical scale of the minimum is less than 100 m.

The NPIW (Fig. 7d) occurs in most of the subtropical gyre. Again, our limited data may not show the complete NPIW region. Talley (1992) describes the NPIW distribution in greater detail.

Since the areas in Figs. 7a and 7c are nearly mutually exclusive, we will find two areas with a triple-salinity minimum when Figs. 7a–c are superimposed on Fig. 7d. The two areas are labeled I and II in Fig. 8. The triple-salinity minimum in area I consists of the SSM, the middle salinity minimum, and the NPIW. The horizontal extent of area I depends mainly on the area

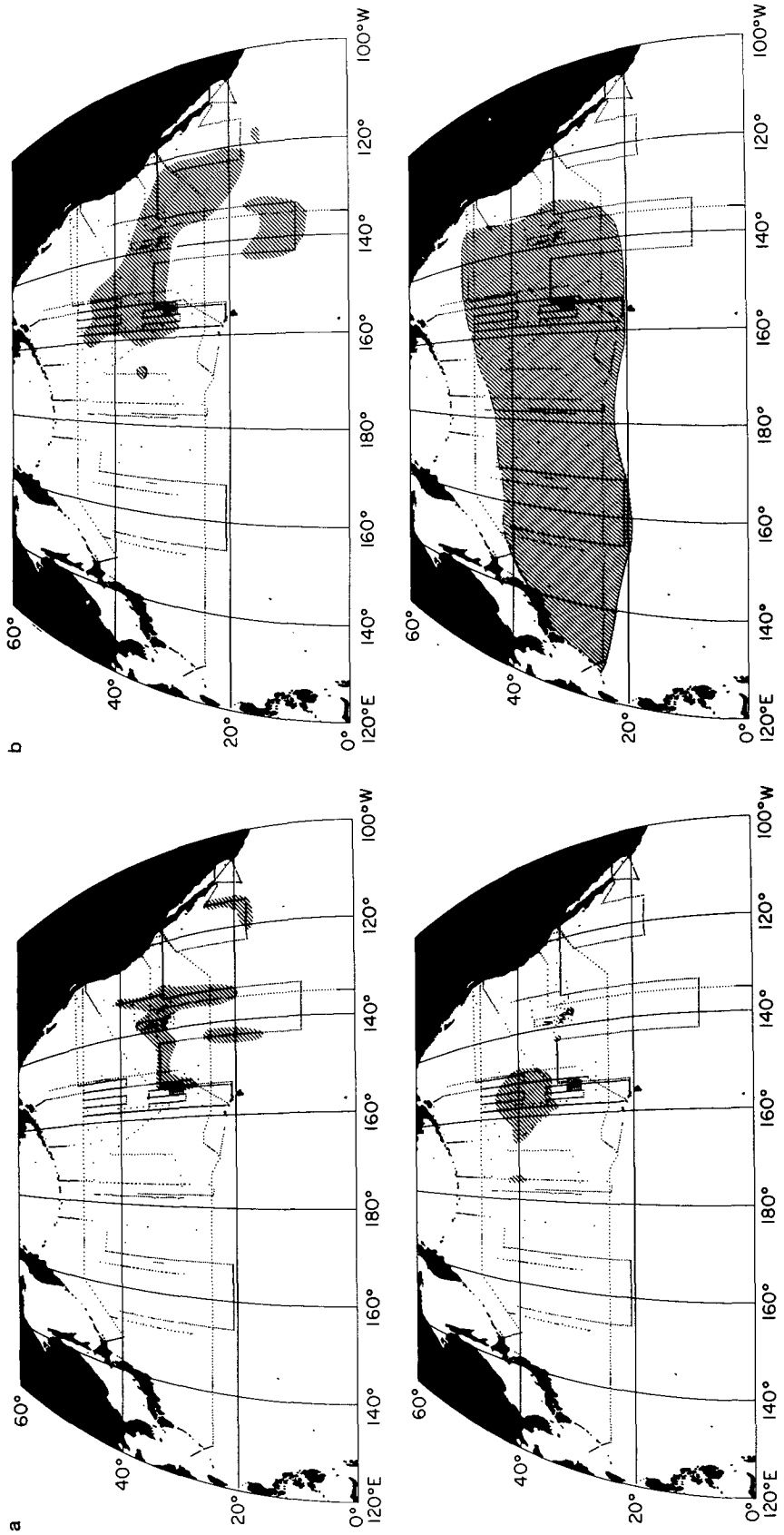

FIG. 7. The shaded areas indicate that salinity minima are found in the density range (a) less than 25.1 σ_θ, (b) between 25.1 and 26.0 σ_θ, (c) between 26.0 and 26.5 σ_θ, and (d) between 26.5 and 26.8 σ_θ. The dots are the data locations for all 24 cruises.

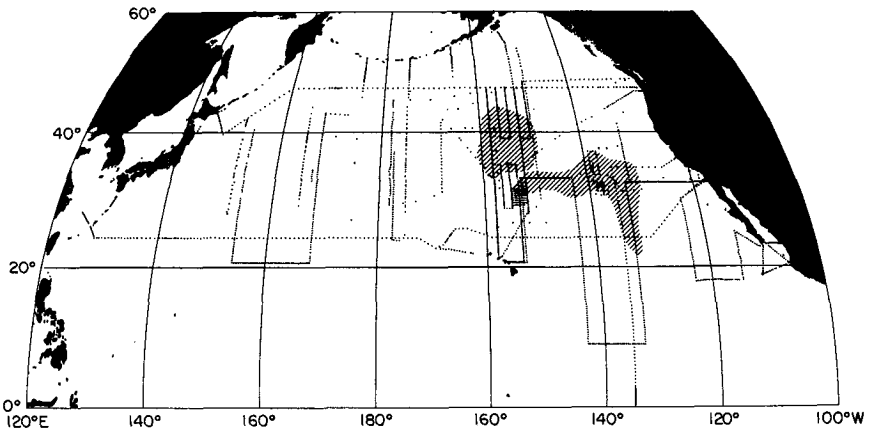

FIG. 8. The triple-salinity minimum has been found in the two shaded areas in the eastern North Pacific. The dots are the data locations for all 24 cruises.

of the middle salinity minimum. The same salinity structure intermittently appears along 35°N from 135° to 158°W in March 1976 (Kenyon 1978b). It also can be traced as far as 28° to 30°N between 155° to 158°W in August 1978 (Hayward and McGowan 1981). The Marathon II minima (Fig. 6) are a good example of the vertical salinity structure during spring in this area. Figure 9a shows the salinity structure in fall in the same area; σ_θ/S relations of seven stations from 39° to 40.5°N along 150°W collected in September 1975 are displayed in Fig. 9a. The middle salinity minimum is found between 26.4 and 26.5 σ_θ, and the NPIW is still between 26.7 and 26.8 σ_θ. The SSM appears in a wider density range between 26.0 and 25.1 σ_θ. In contrast, the middle minimum in both spring and fall occurs in a narrow density range below the permanent pycnocline. The triple-salinity minimum has been found in April 1968, September 1975, July 1983, May 1985, and September 1987, but not in May 1987 in this area. In the data of May 1987, the absence of the SSM left only two minima.

Area II is southeast of area I. The triple-salinity minimum is formed by the seasonal minimum overlying the SSM during summer and fall and the NPIW underlying the SSM. In our data, it starts from 37°N, reaches as far south as 22°N, and is between 154° and 133°W. It is not clear that area II is bounded by any fronts. The shape of area II mainly depends on the seasonal minimum in the available data, which may not represent the true area. In the data of June 1976 σ_θ/S relations along 137.5°W (Lynn 1986) show the typical salinity structure in area II (Fig. 9b). The SSM occurs within the permanent pycnocline rather than below it. Compared with the shallow minimum in area I, the minimum in area II is vertically much smoother and has a wider density range and higher salinity at the minimum. The seasonal salinity minimum is more variable than both the SSM and the NPIW.

A triple-salinity minimum structure has been detected in area I in different seasons and years, convincing us that this phenomenon is not temporary. In area II, the triple-salinity minimum is seasonal, occurring in summer and fall. Both areas of the triple-salinity minimum fall in the area of Reid's SSM (Fig. 8 here; Fig. 1 in Reid 1973). In area I, the density level of the shallowest salinity minimum in winter is consistent with Reid's observations in that area. The middle salinity minimum has not been reported previously. This middle minimum usually does not extend to area II. In area II, the SSM is also similar to Reid's observations, while the seasonal minimum is new to us.

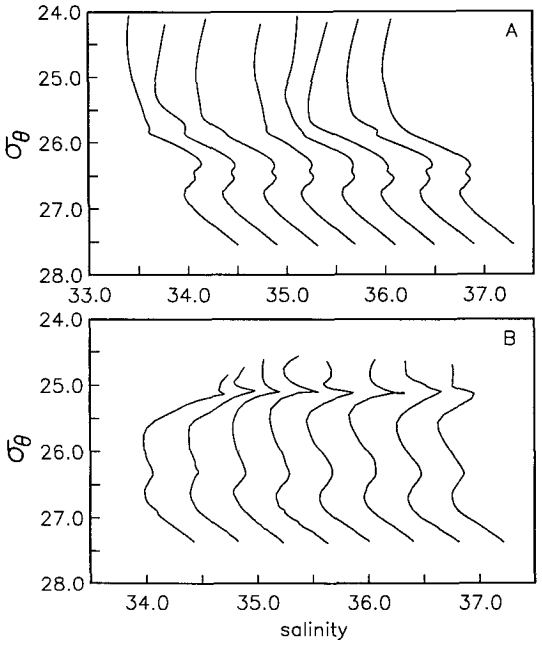

FIG. 9. The σ_θ/S relations (a) from 39° to 40.5°N along 150°W in September 1975 and (b) from 31.7° to 32.5°N along 137.5°W in June 1976.

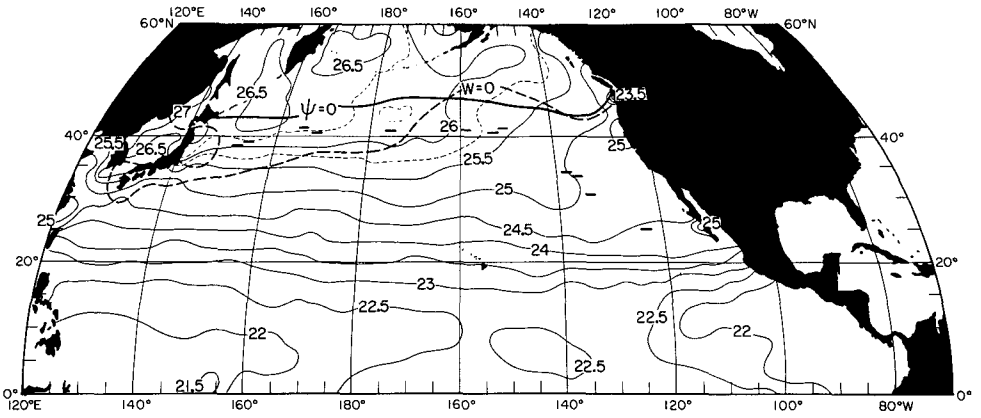

FIG. 10. Surface density in winter from Levitus' (1982) data. The heavy solid line represents the Sverdrup streamfunction $\psi = 0$ and the heavy dashed line represents Ekman pumping $W = 0$. Both are calculated from Hellerman and Rosenstein's (1983) winter (February, March, and April) climatological wind stress. Bars indicate the subarctic front.

The vertical resolution of standard bottle data between 150 and 300 m is 50 m, which is inadequate for resolving phenomena of about 100 m thickness or less. In area I, the shallow minimum lies above 150 m where bottle data have higher vertical resolution. The middle salinity minimum found from CTD/STD data in area I is between 200 and 250 m and is poorly resolved in bottle data. The greatest density at Reid's SSM is 26.2 σ_θ near 25°N, 140°W. We also found salinity minima from CTD/STD sections at this density in this region, as well as minima at lower densities. The isopycnal 26.2 σ_θ lies at approximately 300 m in this region, a standard depth for bottle data.

4. Source waters and lateral circulation of the salinity minima

The source of the SSM has been discussed in previous studies. Stommel (1979) suggested that the winter surface density determines water properties on ventilated isopycnals in the subtropical gyre because of the slowness of advection relative to the peregrinations of surface outcrops. Reid (1973) suggested that surface water at high latitudes is the source of the SSM. Kenyon (1978a) concluded that the source of low-salinity water appears to be in the east based on a zonal STD section at 35°N. By calculating acceleration potential and plotting the depth, salinity, oxygen, and nutrients on 240 cl t^{-1} (25.6 σ_θ), Tsuchiya (1982) pointed out that the low salinity water originates at the sea surface near 35°–50°N, 145°–160°W where the outcrop runs more or less meridionally and that flux of the subarctic low salinity water into the subtropical gyre is limited to the area east of 160°W at this thermosteric anomaly. Talley (1985) used a four-layer model and winter surface conditions to show that the SSM in the eastern Pacific is a feature of the ventilated, wind-driven circulation. Ventilation should occur on all isopycnals outcropping in the northern half of the subtropical gyre. The winter surface salinity in the outcropping zone and wind pattern determine the density layers in which the minimum occurs.

Winter (February, March, and April) surface density from Levitus (1982) is plotted in Fig. 10. The Sverdrup transport streamfunction ψ (including Ekman transport) and the Ekman pumping W are calculated from climatological winter (February, March, and April) wind stress (Hellerman and Rosenstein 1983). $\psi = 0$ and $W = 0$ are superimposed on the winter surface density. The subarctic front (bars in Fig. 10) is between $\psi = 0$ and $W = 0$ west of 170°W and south of $\psi = 0$ and $W = 0$ east of 170°W. The isopycnals of 26.2–26.5 σ_θ outcrop between 165°E and 170°W, the available source water region. The salinity of surface water in this outcrop area north of the SFZ is quite low. South of the SFZ, the surface salinity becomes higher than 34.0 psu west of 170°W (Reid 1969). We therefore regard the SFZ as the southern boundary of the source water. The northern boundary of the source water is suggested to be gyre boundary, $\psi = 0$. From theoretical considerations, the surface water north of $\psi = 0$ will circulate in the subarctic gyre and will not contribute to the salinity minimum in the subtropical gyre. The narrow band between $\psi = 0$ and the SFZ could be the source water area for the middle salinity minimum.

Using a set of high-quality bottle data, including data from J. Reid and A. Mantyla and several recent cruises across the North Pacific, acceleration potentials at 25.6 and 26.2 σ_θ relative to 2000 m are calculated (Fig. 11). The depth of 25.6 σ_θ is greater than 200 m in the central subtropical gyre near 25°N, decreasing both northward and southward, as well as toward the eastern boundary. The depth of 26.2 σ_θ has the same pattern; the greatest depth is more than 400 m near 25°N. In most of the subtropical gyre of the eastern North Pacific, the depth is greater than 200 m. The SSM and the middle salinity

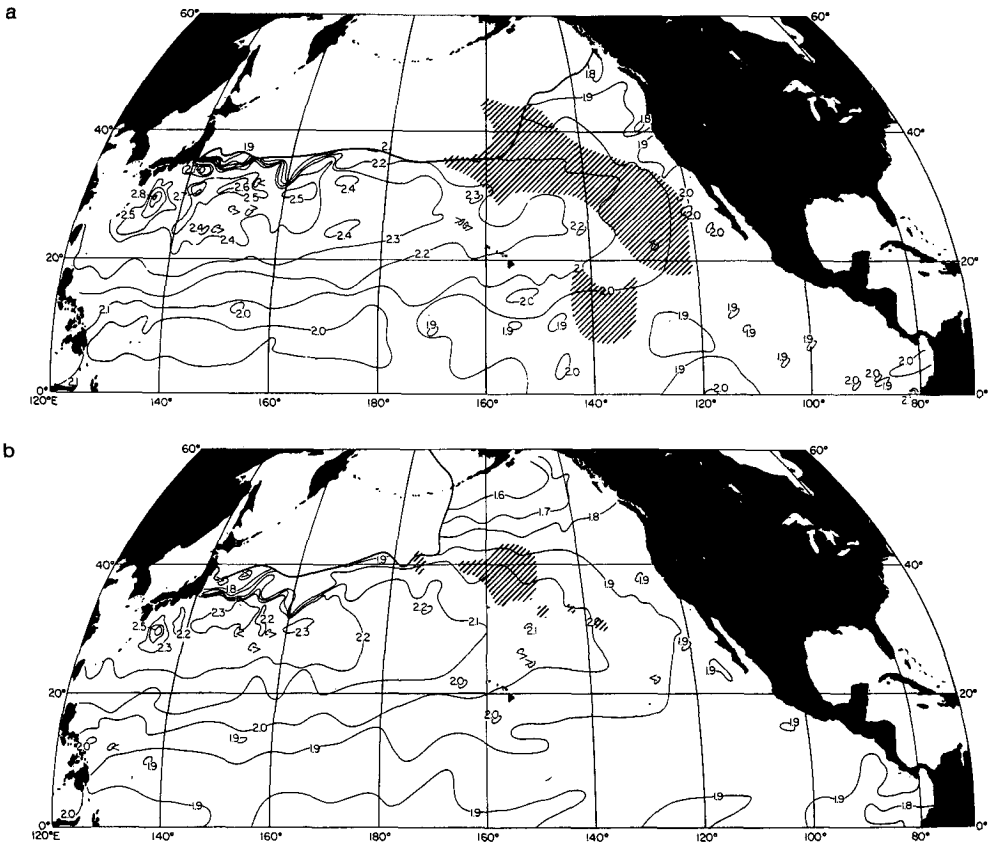

FIG. 11. Acceleration potential in 10 $m^2 s^{-2}$ at (a) 25.6 σ_θ and (b) 26.2 σ_θ relative to 2000 m. The heavy solid lines represent the outcrops of these two isopycnals at the sea surface based on Levitus' (1982) winter surface density. The shaded areas indicate the areas of the shallow and middle salinity minima.

minimum areas are shaded in Figs. 11a and 11b, respectively. Both minima are downstream of their source areas, which implies that geostrophic flow advects the low salinity water southeastward. East of 170°W (in Fig. 11b), we surmise that the southward component of geostrophic flow carries the subducted water on 26.2 σ_θ across the subarctic front from north to south where it meets high salinity surrounding water. This produces the middle salinity minimum in area I.

Figure 12 shows salinity on three isopycnals: 25.6, 26.2, and 26.6 σ_θ. The same depth pattern appears at 26.6 σ_θ as at 25.6 and 26.2 σ_θ. The depth is greater than 300 m in most of the subtropical gyre in the eastern North Pacific. The greatest depth is more than 500 m near 25°N. The salinity distributions clearly show that the subtropical gyre retreats northward with depth (also in Reid and Arthur 1975; Levitus 1982). The low salinity tongue can reach as far south as 10°N at 25.6 σ_θ (Fig. 12a), but it reaches only 20°N at 26.2 σ_θ. At 26.6 σ_θ, the low salinity tongue is limited to north of 30°N. These patterns show why the SSM extends farther south than the middle minimum.

The meridional narrowness of the source area determines the temperature, salinity, and density at the middle minimum. Since the position of the front, surface density, and wind pattern in winter vary interannually, the middle salinity minimum may occur at different densities in different years. Surface heating in the following spring will block further vertical mixing down to the ventilated water. The temperature and salinity of the ventilated water will therefore be advected along the isopycnal without significant change. Because of limited data, the water path cannot be traced from the source area to the region where the middle salinity minimum is found; neither can the southeastern extent of the minimum mentioned in the previous section be traced. The horizontal extent of the middle salinity minimum also varies in different years. The highest density, 26.23 σ_θ (180×10^{-8} m^3 kg^{-1}) at Reid's shallow salinity minimum (Fig. 1 in Reid 1973), occurs from 23° to 28°N, 135° to 145°W. We think that the salinity minimum at this density must have the same source as the middle salinity minimum in area I since this density does not outcrop in the source area of the SSM (Tsuchiya 1982). Because the source area of the middle salinity minimum in area I is rather small, this minimum has a limited vertical scale and cannot be spread over a large horizontal area, making it difficult

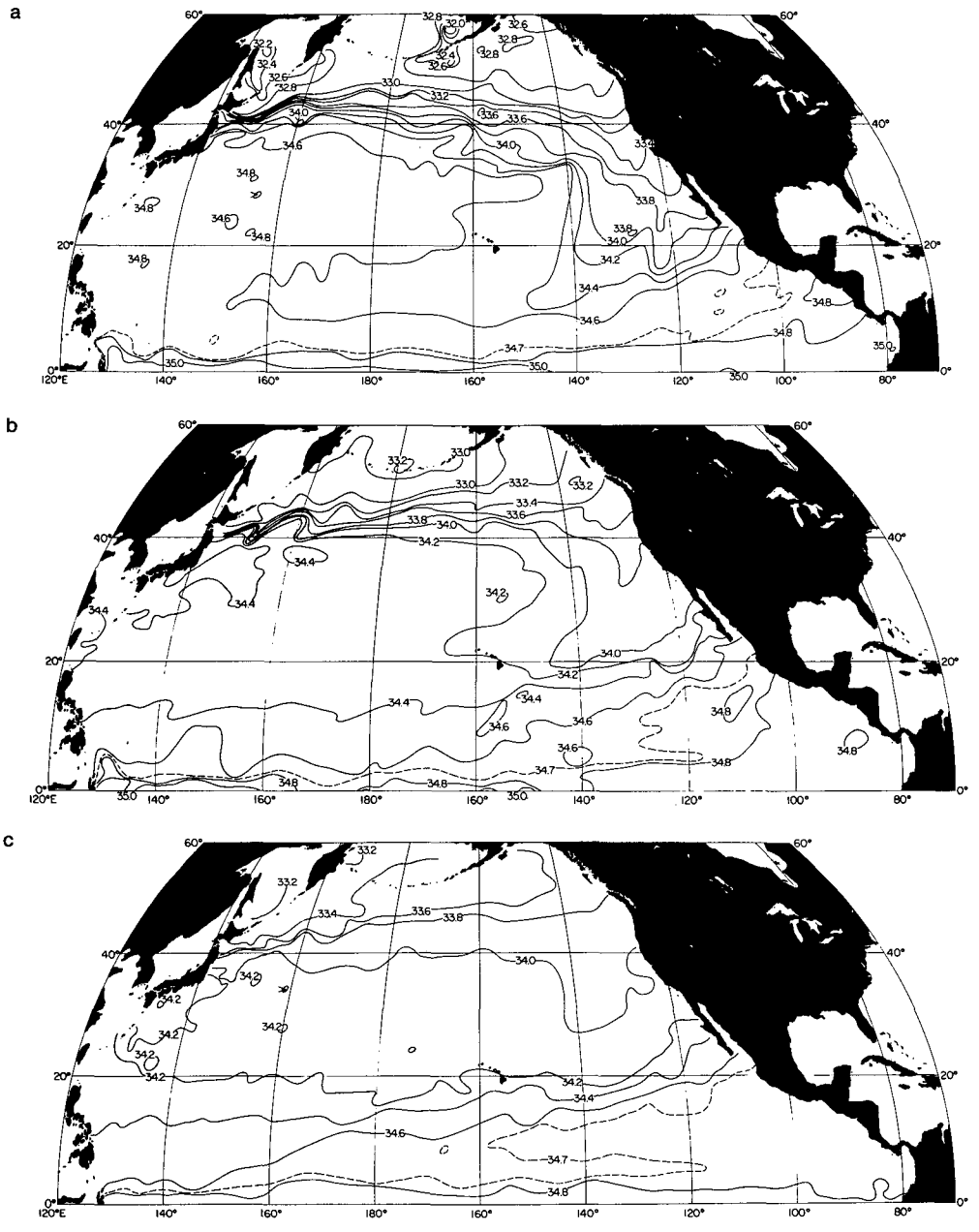

FIG. 12. Salinity at (a) 25.6 σ_θ, (b) 26.2 σ_θ, and (c) 26.6 σ_θ based on the same dataset as Fig. 11.

to find in bottle data. Vertical diffusion will eventually erase it.

The source of low salinity water in the SSM of area I is between 35° and 50°N east of 160°W, as Tsuchiya pointed out in 1982. Ekman pumping is negative (downwelling) in this region so that the minimum is created by direct Ekman subduction in winter and carried by the North Pacific Current and the California Current eastward and southeastward, respectively. Figure 11a confirms this point. The source area of this minimum is larger than that of the middle salinity minimum. Therefore, it is spread over a larger area in the eastern subtropical gyre. Lateral variations in the surface source properties produce the high variability of temperature, salinity, and density at the minimum.

In area II, the middle salinity minimum cannot be found consistently except in a few locations. The SSM stays in the same density range as in area I, so it has the same physical mechanism and the same source. A seasonal minimum above the SSM is produced by Ekman-type subduction in summer and fall. In summer, the surface temperature increases, whereas the salinity does not have much seasonal change (Reid 1969). Surface density, therefore, becomes much lower in summer than in winter (Reid 1969), ranging from 24.0 to 24.5 σ_θ in area II. Downwelling prevails through

most of the year in this area. The mechanism of producing a seasonal minimum is the same as the SSM except it occurs only during summer and fall at much lower densities. Surface cooling in winter destroys the seasonal minimum.

Winter surface density increases and salinity decreases monotonically from south to north (Reid 1969). Why does the low salinity surface water not intrude into the subtropical gyre at every outcropping density layer? The CTD salinity profiles examined here (Fig. 6) suggest that the middle salinity minimum results from the intrusion of low salinity water into the mean salinity maximum of the ambient water. The high salinity at the maximum apparently arises from vertical diffusion from the overlying salinity maximum in the southern subtropical gyre and Kuroshio (Fig. 11 and Fig. 12). The reason for the discreteness of the shallow and middle salinity minima is found in the pattern of the winter surface outcrops relative to the Sverdrup transport and the SFZ (Fig. 10). For instance, upstream of area I, the 26.0 σ_θ outcrop is nearly zonal and south of the SFZ. The surface salinity in the outcropping zone is rather high, so even though the wind forcing ($W < 0$) is favorable to the subduction, the subducted water does not bring low salinity into area I. At 165°W, the 26.0 σ_θ outcrop suddenly turns northward to an area north of the SFZ, where the surface salinity is low and $W < 0$. However, since this part of the outcropping area is directly north of area I, the subducted low salinity water is probably advected east of area I toward the North American coast (Fig. 11b). Thus, the lack of low salinity subducted water leaves a salinity maximum at 26.0 σ_θ in area I. On the other hand, there is also a lack of low salinity water between the middle salinity minimum and the NPIW, between 26.5 and 26.7 σ_θ in area I. These isopycnals, which primarily outcrop in the subpolar gyre, also outcrop in the mixed-water region between the Kuroshio extension and Oyashio Front (Fig. 10) (Talley 1991). The southern part of the outcropping region is thus inside the subtropical gyre where its salinity is increased due to saline surface water introduced by the Kuroshio and Tsugaru Warm Current. If this surface water is subducted and then advected southeastward, it cannot generate a salinity minimum in the subtropical gyre because of its high salinity. Another intriguing possibility is that subduction on these isopycnals does not occur in the subtropical gyre since $W > 0$ in their outcropping area (Fig. 10).

Ventilation is assumed to occur on all isopycnals that outcrop in the northern half of the subtropical gyre if $W < 0$. The vertical salinity minima in the subtropical gyre can be regarded as a tracer of this ventilation. However, only ventilation on the isopycnals that outcrop in the areas of relatively low surface salinity (such as north of the SFZ) will generate vertical salinity minima in the subtropical gyre. So the minima do not represent all ventilation. Amounts of low salinity water intruded into the subtropical gyre along the isopycnals depend on the size of the source area and whether there is Ekman pumping or suction. The source area of the middle salinity minimum is rather narrow, and the wind pattern does not always produce Ekman pumping, which is a direct mechanism for subduction, in the source area. Therefore, the middle salinity minimum is found in a relatively small area. On the other hand, the SSM represents the majority of the low salinity water flushing into the subtropical gyre from north above the NPIW since its source area is relatively large and Ekman pumping prevails in the area.

5. Tropical salinity minimum

Reid (1973) showed that the SSM turns southwestward with the eastern boundary current near 20°N and spreads between 10° and 20°N from 130° to 170°W in the density range of 25.4 to 25.7 σ_θ. Emery and Dewar (1982) showed in their mean temperature and salinity curves that there are multiple salinity minima in the same region. Two of them are more profound than the others. One occurs at 26.0 σ_θ, and the other is the Antarctic Intermediate Water (AAIW) with density greater than 27.0 σ_θ. There are also some weak minima above 25.0 σ_θ. Emery and Dewar claimed that the presence of a variety of intermediate waters causes the multiple salinity minima.

Figure 7b shows a separate shallow salinity minimum south of 20°N near 140°W, which we call the tropical salinity minimum. It occurs at about 26.0 σ_θ and from 8° to 18°N, 130° to 145°W. There is not enough data to determine whether this minimum is connected to the SSM east of 130°W. This minimum is observed at least as far west as 150°W (Talley, personal communication). A CTD section (WOCE P17) along 135°W occupied in summer 1991 gives a good demonstration of the evolution of vertical salinity structure from north to south in this area. The σ_θ/S relations from every other station from stations 22 to 76, which cover 32°–5°N, are plotted in Fig. 13. Figure 13a shows σ_θ/S relations in the subtropical gyre from 32° to 26°N (from left to right). The SSM occurs at 26.0 σ_θ or above, and the NPIW is at 26.8 σ_θ. There is a salinity maximum between the SSM and the NPIW with a salinity of 34.1 psu. The two salinity minima become weaker southward as they are farther away from their source regions. Vertical mixing tends to smooth out the maximum. The two salinity minima merge together in Fig. 13b, which covers latitudes from 25° to 19°N along 135°W. High salinity of the surface water results from excess evaporation. The underlying low salinity water mass is about 300 m thick and becomes thinner to the south. A high salinity intrusion at 26.6 σ_θ breaks the ambient low salinity water. The intrusion starts at about 16°N (station 54 in Fig. 13c) and becomes stronger southward. The salinity at the saline intrusion is 34.7 psu, which is much higher than the salinity in the maximum between the SSM and the NPIW in the subtropical gyre. Now a shallow salinity minimum (a "tropical salinity minimum" to distin-

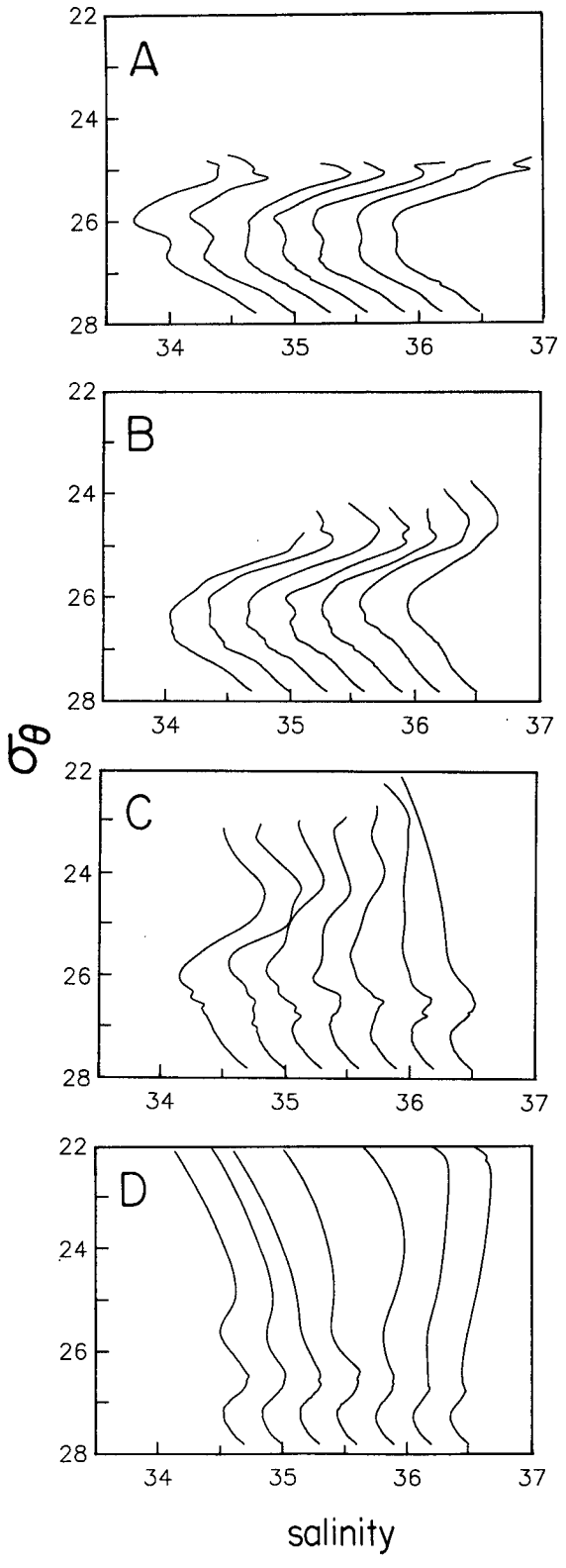

FIG. 13. The σ_θ/S relations for every 1° latitude along 135°W in June 1991. (a) Stations from 32° to 26°N (from left to right, same in the following panels), (b) from 25° to 19°N, (c) from 18° to 12°N, and (d) from 11° to 5°N.

guish it from the SSM in the subtropical gyre) reappears at 26.0 σ_θ while the salinity maximum is developing. Meanwhile, below the high salinity intrusion, the AAIW with low salinity advects into this area below 27.0 σ_θ. Two salinity minima then are established—the tropical salinity minimum and AAIW minimum. It is also noted that the surface salinity decreases southward in the intertropical zone.

The same vertical salinity evolution from north to south was found in October 1972 along 143° and 133°W (Roden 1974). There is a gap between the SSM and the tropical salinity minimum in both sections. We suggest that the high salinity intrusion at 26.6 σ_θ creates the tropical salinity minimum above it. The salinity distribution at 26.6 σ_θ (Fig. 12c) shows clearly that the high salinity comes from the equatorial region east of 120°W. A high salinity tongue indicated by 34.7 psu extends westward along 10°N. Tsuchiya (1968) first noticed this high salinity tongue and its corresponding vertical salinity maximum. He suggested that the source of the high salinity is east of 115°W where a vertical salinity maximum exists. The high salinity water is advected westward by the southern part of the North Equatorial Current. A low oxygen tongue accompanies the high salinity tongue, which confirms the source.

We think that the tropical salinity minimum may not be the continuation of the SSM. Through vertical mixing, the SSM and the NPIW gradually lose their identity near 20°N west of 130°W, resulting in a single smooth and thick low salinity water mass between 25.1 σ_θ and 27.0 σ_θ. The water of the tropical minimum originates from this thick minimum. The high salinity water advected from east of 115°W breaks the low salinity water mass and creates the tropical salinity minimum above it. Therefore, the mechanism of forming the tropical minimum differs from that of the SSM.

6. Discussion

We have discussed the source area of the middle salinity minimum and where the low salinity is advected in the subtropical gyre. However, how the low salinity surface water subducts and feeds into the general circulation below the mixed layer still remains unknown from a theoretical point of view. Following are a few possible subduction scenarios. The Luyten et al. (1983) model assumes zonal outcrops and zonal winds and ignores the Ekman flow except as it produces Sverdrup transport through its convergence. Subduction occurs only in the subtropical gyre where there is Ekman downwelling. Talley (1985) modified this model slightly to take account of nonzonal winds but did not look at solutions in the interesting region between $\psi = 0$ and $W = 0$ (Fig. 10) where there is upwelling in the subtropical gyre. In the actual source area in the subtropical gyre for the middle salinity minimum, the winds are nonzonal and there is usually Ekman up-

welling; flow here cannot subduct until the flow paths cross into the area where there is Ekman downwelling (see Fig. 10). The actual surface currents in this area are nearly zonal (Wyrtki 1975). Surface water is transported eastward until 170°W, where the isopycnal outcrops run more or less meridionally and Ekman pumping also changes sign; subduction then becomes possible. A difficulty with this picture is that the actual average surface density in the source region decreases to the east, so if flow is nearly zonal, density would need to decrease along the path, requiring either freshwater input or heating.

Huang's (1987) three-layer model suggested a more complicated subduction process in the northern subtropical gyre. In his supercritical state, wind forcing is strong enough to make the second layer outcrop. The outcropping area can extend south of the zero wind-curl line into the subtropical gyre. The second layer is driven directly by wind forcing in the outcropping area. There is a strong cross-gyre exchange in this state. Subtropical water flows northward into the subpolar gyre in the top layer. Consequently, the second layer is forced to move southward across the zero wind-curl line into the subtropical gyre. If there is outcropping within the subtropical gyre but north of the SFZ, low salinity surface water will be transported southward in the second layer where it could become a subducted salinity minimum.

Time dependence of the winds, including both annual and interannual changes, may also permit subduction of the low salinity waters in the northern subtropical gyre even though the average Ekman pumping is upward in the apparent source region. If Ekman pumping is dominant during some part of the year, subduction could occur. Han and Lee's (1981) average monthly wind stress curl shows the Ekman upwelling extending well south of our winter average $W = 0$ in January and February; the March pattern is similar to the winter average, and in April the downwelling region extends northward, north of our $W = 0$. This persists until September. Thus, the Ekman pumping pattern at the end of winter (April) is favorable for subduction of the low salinity surface water north of the subarctic front. A full theory of subduction with time-dependent, nonzonal winds is lacking and would be appropriate for understanding creation of the middle salinity minimum. Thus, variations of wind forcing, circulation, and winter surface density could produce a middle salinity minimum at different densities between 26.0 σ_θ and the NPIW in different years. In some years, such as the survey in September 1982, there may even be no formation of the middle salinity minimum.

These three models do not include explicit southward flow of the Ekman layer, which brings relatively fresh, subpolar surface water into the subtropical gyre. They also do not include the subarctic front, which is an apparent barrier to free flow of the Ekman layer and which appears to be the northern limit of the middle salinity minimum. A full ventilation theory should also include these elements.

7. Summary

The salinity minima in the North Pacific indicate water exchange between the subpolar and the subtropical gyres. Low salinity surface water in the northern outcropping zone may be subducted by Ekman pumping and then advected by geostrophic flow along isopycnals. Depending on the surface conditions, more low salinity surface water is advected on some isopycnals than others into the eastern North Pacific. When the ventilated water meets high salinity water in the subtropical gyre, vertical salinity minima are formed on these isopycnals. The requisite surface conditions for formation of the minima are: the isopycnals outcrop more or less meridionally in the northern subtropical gyre, surface salinity is low in the outcropping region, and there is Ekman downwelling in the outcropping region. Since the subtropical gyre shifts poleward with depth, the water at lower densities will be advected farther southeastward than at greater densities. Both the middle and shallow salinity minima, as well as the seasonal salinity minimum, are likely to be produced by this Ekman-type subduction. The importance of the subarctic front in production of the sharp salinity minima is apparent from the CTD data presented in this paper, but how the front fits into general circulation/ventilation theory is unknown. The mechanism for forming the NPIW salinity minimum also appears to involve "subduction" at the Oyashio front close to Japan (Talley 1992), but subduction there arises from the southward penetration of the front itself rather than from southward advection (Ekman and geostrophic) across the subarctic front.

The middle salinity minimum in area I occurs at the greatest densities that outcrop in winter in the subtropical gyre. It appears below the permanent pycnocline at a depth of about 250 m. The thickness of the minimum is less than 100 m, requiring data with high vertical resolution for identification. The source of the middle minimum is the surface water west of 170°W, bounded by the gyre boundary and the SFZ. The source is limited by the narrowness of the region and intermittence of Ekman downwelling due to the annual wind stress cycle in the source region. Thus, this minimum does not spread over a large area in the eastern North Pacific. On the other hand, the narrowness of the source region narrows the minimum's density range. Since the minimum is found rather near the source region, it appears as a new intrusion with a sharp shape in the σ_θ/S relation.

The SSM is formed in winter and can be detected in all other seasons. The minimum usually occurs within the permanent pycnocline in the density range between 25.1 to 26.0 σ_θ. The source area of the minimum is between 35° and 50°N east of 160°W. Since the source area is relatively large and Ekman pumping

prevails in the source area, this minimum spreads over a large area in the eastern boundary current region.

The surface density becomes much lower in summer due to heating. In area II, a seasonal salinity minimum is formed above the SSM in summer and fall. It is in the density range above 25.1 σ_θ, which is usually in the mixed layer. Surface cooling in winter apparently destroys the minimum.

A tropical salinity minimum is found south of 20°N, separated from the SSM. When mixing gradually destroys the separate identities of the SSM and the NPIW, a thick, low salinity water mass is formed between 25.0 and 27.0 σ_θ in the south. High salinity water is advected along 10°N at about 200 m into this low salinity water mass. A vertical salinity maximum is then created at 26.6 σ_θ, which thus creates a minimum at 26.0 σ_θ. The density range of the tropical minimum is the same as that of the shallow minimum, while the salinity at the tropical minimum is higher than that of the shallow minimum.

Acknowledgments. We are grateful to G. Roden, R. Lynn, P. Niiler, T. Joyce, D. Roemmich, and P. Worcester for providing CTD/STD data for this research. J. Reid provided bottle data. R. deSzoeke was chief scientist for the Marathon II cruise and M. Tsuchiya for the WOCE P17 cruise. Discussions with J. Reid, M. Tsuchiya, P. Bogden, and B. Dushaw and the comments from Y. Nagata were very helpful. Our special thanks go to the anonymous reviewers whose careful and detailed comments helped improve the manuscript greatly. This research was supported by the National Science Foundation, Ocean Science Division, through Grant OCE87-58120.

REFERENCES

Emery, W. J., and J. S. Dewar, 1982: Mean temperature–salinity, salinity–depth and temperature–depth curves for the North Atlantic and the North Pacific. *Progress in Oceanography,* Vol. 11, Pergamon, 219–305.

Han, Y.-J., and S.-W. Lee, 1981: A new analysis of monthly mean wind stress over the global ocean. Climatic Research Institute and Department of Atmospheric Sciences, Oregon State University, Report No. 26, 151 pp.

Hasunuma, K., 1978: Formation of the intermediate salinity minimum in the northwestern Pacific Ocean. *Bull. Ocean Res. Inst. University of Tokyo,* **9,** 1–47.

Hayward, T. L., and J. A. McGowan, 1981: The shallow salinity minimum and variance maximum in the central North Pacific. *Deep-Sea Res.,* **28A,** 1131–1146.

Hellerman, S., and M. Rosenstein, 1983: Normal monthly wind stress over the World Ocean with error estimates. *J. Phys. Oceanogr.,* **13,** 1093–1104.

Huang, R. X., 1987: A three-layer model for wind-driven circulation in a subtropical–subpolar basin. Part II: The supercritical and hypercritical states. *J. Phys. Oceanogr.,* **17,** 679–697.

Kenyon, K. E., 1978a: The shallow salinity minimum of the eastern North Pacific in winter. *J. Phys. Oceanogr.,* **8,** 1061–1069.

——, 1978b: Physical, Chemical and Biological data. INDOPAC Expedition, SIO Reference 78-21, 424 pp.

Kitani, K., 1973: An oceanographic study of the Okhotsk Sea—particularly in regard to cold waters. *Bull. Far Seas Fish. Res. Lab.,* **9,** 45–77.

Joyce, T. W., 1987: Hydrographic sections across the Kuroshio extension at 165°E and 175°W. *Deep-Sea Res.,* **34,** 1331–1352.

Levitus, S., 1982: *Climatological Atlas of the World Ocean.* NOAA Prof. Paper 13.

Luyten, J. R., J. Pedlosky, and H. Stommel, 1983: The ventilated thermocline. *J. Phys. Oceanogr.,* **13,** 292–309.

Lynn, R. J., 1986: The subarctic and northern subtropical fronts in the eastern North Pacific Ocean in spring. *J. Phys. Oceanogr.,* **16,** 209–222.

Martin, M., L. D. Talley, and R. A. de Szoeke, 1987: Physical, chemical and CTD data from the Marathon Expedition, *R/V Thomas Washington* 261, Oregon State University, Ref. 87–15, 213 pp.

Niiler, P. P., 1986: Pacific thermocline circulation study. Scripps Institution of Oceanography Ref. 86-27, 132 pp.

——, W. J. Schmitz, and K. D. Lee, 1985: Geostrophic volume transport in high eddy-energy areas of the Kuroshio extension and Gulf Stream. *J. Phys. Oceanogr.,* **15,** 825–843.

Reid, J. L., 1965: Intermediate waters of the Pacific Ocean. *Johns Hopkins Oceanographic Studies,* No. 2, 85 pp.

——, 1969: Sea-surface temperature, salinity, and density of the Pacific Ocean in summer and in winter. *Deep-Sea Res.,* **16**(Suppl.), 215–224.

——, 1973: The shallow salinity minima of the Pacific Ocean. *Deep-Sea Res.,* **20,** 51–68.

——, and R. S. Huther, 1975: Interpretation of maps of geopotential anomaly for the deep Pacific Ocean. *J. Mar. Res.,* **33**(Suppl.), 37–52.

Roden, G. I., 1970: Aspects of the mid-Pacific transition zone. *J. Geophys. Res.,* **75,** 1097–1109.

——, 1972: Temperature and salinity fronts at the boundary of the subarctic–subtropical transition zone in the western Pacific. *J. Geophys. Res.,* **77,** 7175–7187.

——, 1974: Thermohaline structure, fronts, and sea–air energy exchange of the trade wind region east of Hawaii. *J. Phys. Oceanogr.,* **4,** 168–182.

——, 1977: Oceanic subarctic fronts of the central Pacific: Structure of and response to atmospheric forcing. *J. Phys. Oceanogr.,* **7,** 761–778.

——, 1980: On the subtropical frontal zone north of Hawaii during winter. *J. Phys. Oceanogr.,* **10,** 342–362.

Roemmich, D. H., J. H. Swift, R. F. Weiss, and H. G. Ostlund, 1990: Physical, chemical, and CTD data report S.I.O. Ref. 90-36, 463 pp.

Stommel, H., 1979: Determination of water mass properties of water pumped down from the Ekman layer to the geostrophic flow below. *Proc. Natl. Acad. Sci. USA,* **76,** 3051–3055.

Talley, L. D., 1985: Ventilation of the subtropical North Pacific: The shallow salinity minimum. *J. Phys. Oceanogr.,* **15,** 633–649.

——, 1991: An Okhotsk Sea water anomaly: Implications for ventilation in the North Pacific. *Deep-Sea Res.,* **38,** 171–190.

——, 1992: Distribution and formation of North Pacific Intermediate Water. *J. Phys. Oceanogr.*

——, M. Martin, and P. Salameh, 1988: *Transpacific section in the subpolar gyre.* S.I.O. Ref. 88-9, 245 pp.

——, T. M. Joyce, and R. A. de Szoeke, 1991: Transpacific sections at 47°N and 152°W: Distribution of properties. *Deep-Sea Res.,* **38,** 563–582.

Teague, W. J., 1983: CTD profiles in the Northeast Pacific August–October 1982. Ocean measurement program, U.S. Naval Oceanographic Office, NSTL Station, 335 pp.

Tsuchiya, M., 1968: Upper waters of the intertropical Pacific Ocean. The Johns Hopkins Oceanographic Studies, No. **4,** 50 pp.

——, 1982: On the Pacific upper-water circulation. *J. Mar. Res.,* **40**(Suppl.).

Warren, B. A., and W. B. Owens, 1988: Deep currents in the central subarctic Pacific Ocean. *J. Phys. Oceanogr.,* **18,** 529–551.

Wüst, G., 1930: Meridionale Schichtung und Tiefenzirkulation in den Westhälften der drei Ozeane. *J. Cons. Int. l'Expl. Mer,* **5**(1), 21 pp.

Wyrtki, K., 1975: Fluctuations of the dynamic topography in the Pacific Ocean. *J. Phys. Oceanogr.,* **5,** 450–459.